

# Monolayer Behavior of NBD-Labeled Phospholipids at the Air/Water Interface

Valeria Tsukanova,<sup>†,‡</sup> David W. Grainger,<sup>§</sup> and Christian Salesse<sup>\*,†</sup>

GREIB, Département de Chimie-Biologie, Université du Québec à Trois-Rivières, Trois-Rivières, Québec, Canada G9A 5H7, CERSIM, Université Laval, Ste-Foy, Québec, Canada G1K 7P4, and Department of Chemistry, Colorado State University, Fort Collins, Colorado 80523-1872

Received February 8, 2002. In Final Form: April 26, 2002

Monolayer behavior of the dye 7-nitro-2-1,3-benzoxadiazol-4-yl (NBD)-labeled analogues of phospholipids 1,2-dipalmitoyl-*sn*-glycero-3-phosphatidylethanolamine (DPPE) and 1,2-dipalmitoyl-*sn*-glycero-3-phosphatidylcholine (DPPC) were studied by a variety of methods. Attachment of the NBD chromophore onto either the phospholipid headgroup or the aliphatic chain significantly changes the parent phospholipid monolayer properties. In contrast to that of the condensed-type DPPE monolayer, the isotherm of the DPPE-NBD derivative with NBD in the headgroup exhibits a liquid-expanded/liquid-condensed phase transition plateau while the isotherm of the acyl-chain-labeled NBD(C<sub>12</sub>)-PC shows liquid-expanded behavior lacking the plateau observed in the isotherm of DPPC. Surface potential and spectroscopic data revealed that the NBD group on both DPPE-NBD and NBD(C<sub>12</sub>)-PC embeds into the phospholipid headgroup region of the monolayer, thus suggesting a looping of the NBD-labeled chain of NBD(C<sub>12</sub>)-PC toward water. Polarized fluorescence and red-edge excitation shift studies revealed a regular alignment of uniformly oriented NBD chromophores in the DPPE-NBD monolayer controlled by networks of intermolecular hydrogen bonds. By contrast, the NBD group on NBD(C<sub>12</sub>)-PC experienced a less-structured environment permitting rotation of the NBD chromophore and fast relaxation of surrounding water dipoles. Organization of the NBD-labeled phospholipids at the air/water interface and intermolecular interactions responsible for the monolayer structuring are discussed.

## 1. Introduction

Phospholipids covalently derivatized with dye chromophores are popular probes for fluorescence imaging and photochemistry studies on surfactant, colloidal, interfacial, and membrane systems. Several phospholipids are commercially available with covalently attached 7-nitro-2-1,3-benzoxadiazol-4-yl (NBD) groups. They have been widely used over the last three decades as fluorescent analogues of native phospholipids to study the properties, spatial organization, and distribution of phospholipids and proteins in monolayers, bilayers, and biological membranes.<sup>1–16</sup> As the NBD chromophore may be attached to either the phospholipid polar headgroup or apolar aliphatic

chain in various phospholipid molecules, NBD-based local “reporting” of molecular environments from these analogues is considered advantageous to gain information on phospholipid membrane aggregation and lateral phase separation,<sup>9,11</sup> monolayer organization,<sup>11,12,14</sup> phospholipid domains,<sup>11–13</sup> membrane fusion,<sup>1,4</sup> bilayer-to-hexagonal phase transitions in liposomes,<sup>8</sup> and many other processes by monitoring changes in the photophysical behavior of NBD. In particular, the intrinsic solvatochromic properties of NBD make this chromophore suitable to probe the local polarity of different regions of monolayers and bilayers as well as to study the distribution of phospholipids in model membranes.<sup>1,6,10,17</sup> Nonetheless, several studies revealed that NBD's strong preference for a more-polar environment could induce looping of the NBD-labeled acyl chain toward the aqueous phase.<sup>1,3,6,10</sup> Consequently, systematic differences in polarity detected by acyl-chain-labeled NBD-phosphatidylcholines or NBD-phosphatidylethanolamines compared to other acyl-chain-labeled dye phospholipids were attributed to this possibility. Thus, to avoid misinterpretation of experimental data, knowledge of the actual dye probe environment and dynamics of NBD partitioning between apolar and polar phases must be considered more carefully.

Despite the popularity of this probe and the number of studies in which NBD-labeled phospholipids are routinely used, little attention has been directed to what extent the presence of the NBD chromophore in the phospholipid molecular structure alters their monolayer properties. No

\* To whom correspondence should be addressed. E-mail: christian\_salesse@uqtr.ca.

<sup>†</sup> Université du Québec à Trois-Rivières and Université Laval.

<sup>‡</sup> On leave from the Department of Chemistry, St. Petersburg State University, Petrodvorets, St. Petersburg 198904, Russia.

<sup>§</sup> Colorado State University.

(1) Chattopadhyay, A. *Chem. Phys. Lipids* **1990**, *53*, 1.

(2) Chattopadhyay, A.; Mukherjee, S. *Biochemistry* **1993**, *32*, 3804.

(3) Mazères, S.; Schram, V.; Tocanne, J.-F.; Lopez, A. *Biophys. J.* **1996**, *71*, 327.

(4) Morris, S. J.; Bradley, D.; Blumenthal, R. *Biochim. Biophys. Acta* **1985**, *818*, 365.

(5) Homan, R.; Eisenberg, M. *Biochim. Biophys. Acta* **1985**, *812*, 485.

(6) Huster, D.; Müller, P.; Arnold, K.; Herrmann, A. *Biophys. J.* **2001**, *80*, 822.

(7) Lin, S.; Struve, W. S. *Photochem. Photobiol.* **1991**, *54*, 361.

(8) Hong, K.; Baldwin, P. A.; Allen, T. M.; Papahadjopoulos, D. *Biochemistry* **1988**, *27*, 3947.

(9) Gutiérrez-Merino, C.; Bonini de Romanelli, I. C.; Pietrasanta, L. I.; Barrantes, F. J. *Biochemistry* **1995**, *34*, 4846.

(10) Chattopadhyay, A.; London, E. *Biochim. Biophys. Acta* **1988**, *938*, 24.

(11) McConnell, H. M.; Keller, D.; Gaub, H. J. *Phys. Chem.* **1986**, *90*, 1717.

(12) Flörsheimer, M.; Möhwald, H. *Chem. Phys. Lipids* **1989**, *49*, 231.

(13) Nag, K.; Keough, M. W. *Biophys. J.* **1993**, *65*, 1019.

(14) Nag, K.; Perez-Gil, J.; Ruano, M. L. F.; Worthman, L. A. D.; Stewart, J.; Casals, C.; Keough, M. W. *Biophys. J.* **1998**, *74*, 2983.

(15) Shrive, J. D. A.; Brennan, J. D.; Brown, R. S.; Krull, U. J. *Appl. Spectrosc.* **1995**, *49*, 304.

(16) Brown, R. S.; Brennan, J. D.; Krull, U. J. *J. Chem. Phys.* **1994**, *100*, 6019.

(17) Chattopadhyay, A.; London, E. *Biochemistry* **1987**, *26*, 39.

systematic studies of the monolayer behavior of NBD-labeled analogues of phosphatidylcholine and phosphatidylethanolamine have been reported. However, such a study could provide several important, new sets of information, in particular (1) how the photophysical properties of NBD respond to local changes in polarity and intermolecular interactions as molecules are brought into close contact by monolayer compression and (2) an understanding of the fundamental organizational properties of NBD-phospholipid probes at the air/water interface. The latter is, undoubtedly, important for correct use of NBD-labeled analogues to elucidate mechanisms of membrane processes, membrane structures, and dynamics.

In this paper, we report monolayer behavior for both headgroup-labeled NBD-dipalmitoylphosphatidylethanolamine (DPPE-NBD) and the acyl-chain-labeled NBD-dipalmitoylphosphatidylcholine (NBD(C<sub>12</sub>)-PC). As it remains unclear whether looping of the NBD-labeled acyl chain of NBD(C<sub>12</sub>)-PC occurs in monolayers at the air/water interface and what influences result, localization of the NBD group was assessed through comparative analysis of surface potential data for NBD-labeled and parent phospholipid monolayers based on the Demchak–Fort model.<sup>18–23</sup> Surface potential data also provide evidence about the electrostatics of the NBD-phospholipid/water interface, which are of particular interest in the case of DPPE-NBD, as substitution of two amine protons of the phosphatidylethanolamine group by NBD alters the headgroup charge. To obtain further evidence on the localization of the NBD group and to characterize the spectroscopic properties of DPPE-NBD and NBD(C<sub>12</sub>)-PC in monolayers, in situ absorption and fluorescence spectra measurements were performed at the air/water interface. To gain detailed information on the intermolecular interactions and structural ordering of the NBD-phospholipid monolayers, polarized fluorescence and red-edge excitation shift (REES) effects were measured. The REES effect is usually observed when the mobility of a chromophore relative to the surrounding matrix is considerably reduced.<sup>2</sup> Thus, REES may serve as an indicator of chromophore local environment and has been shown to be a powerful tool in probing interfacial organization.<sup>2</sup>

## 2. Experimental Section

**2.1. Materials.** NBD-labeled phospholipids 1,2-dipalmitoyl-*sn*-glycero-3-phosphatidylethanolamine-*N*-(7-nitro-2,1,3-benzoxadiazol-4-yl) (DPPE-NBD) and 1-palmitoyl-2-[12-[(7-nitro-2,1,3-benzoxadiazol-4-yl)amino]dodecanoyl]-*sn*-glycero-3-phosphatidylcholine (NBD(C<sub>12</sub>)-PC) as well as the parent phospholipids 1,2-dipalmitoyl-*sn*-glycero-3-phosphatidylethanolamine (DPPE) and 1,2-dipalmitoyl-*sn*-glycero-3-phosphatidylcholine (DPPC) were purchased from Avanti Polar Lipids (Birmingham, AL). The chemical structures of these compounds are presented in Figure 1. Spreading solutions of both NBD-labeled and parent phospholipids were prepared with HPLC grade chloroform at typical concentrations of 0.4 mg/mL and stored in glass vials wrapped in aluminum foil in the dark at 4 °C. In all experiments, unless mentioned otherwise, deionized water produced by a Nanopure water purification system was used as the subphase. The specific resistivity of water was  $18 \times 10^6 \Omega \cdot \text{cm}$  (pH 5.6 in

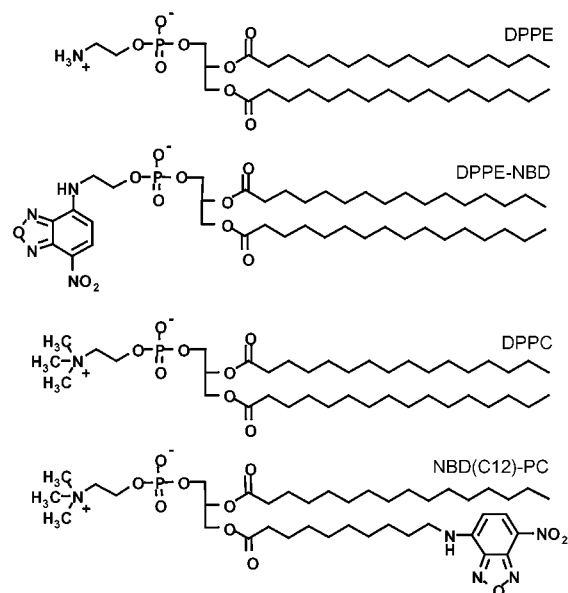


**Figure 1.** Chemical structures of the studied phospholipid molecules.

equilibrium with atmospheric carbon dioxide). Inorganic reagents HCl and CuSO<sub>4</sub> used in the experiments were of AnalaR grade (Omega, QC).

**2.2. Methods.** A homemade Teflon-coated Langmuir trough with a movable barrier described elsewhere<sup>24</sup> was used to study the phospholipid monolayers. The trough was thermostated and enclosed in a box. A filter paper Wilhelmy plate was used to measure surface pressure ( $\pi$ ). Monolayer surface potential ( $\Delta V$ ) was detected with an <sup>241</sup>Am-coated ionizing electrode located 2 mm above the water surface while the reference electrode made of platinum was immersed at the bottom of the trough. During monolayer compression,  $\pi$  and  $\Delta V$  were recorded simultaneously. Surface pressure was detected to an accuracy of 0.1 mN/m, while surface potential was measured to an accuracy of  $\pm 15$  mV.

The trough was also interfaced with an epifluorescence microscope described previously.<sup>25</sup> Epifluorescence micrographs were captured from different regions of the NBD-phospholipid isotherms. The filter set used to observe the NBD fluorescence was a combination of a blue excitation filter (Nikon, M 420-490), a dichroic mirror (Nikon, DM 510), and a barrier filter (Nikon, M 520). Excitation light was focused on the monolayer with a 20 $\times$  objective (Nikon, MPlan 20).

In situ measurements of the absorption and emission spectra at the air/water interface were performed with the trough described by Gallant et al.<sup>26</sup> To measure the quenching of the NBD(C<sub>12</sub>)-PC fluorescence with Cu<sup>2+</sup> ion, an NBD(C<sub>12</sub>)-PC monolayer spread on water was compressed to an area of 0.5 nm<sup>2</sup>/molecule and then 10 mM CuSO<sub>4</sub> solution was injected into the subphase underneath the monolayer to achieve a final subphase concentration of approximately 300–400  $\mu\text{M}$  Cu<sup>2+</sup> ion. After the addition of the quenching agent, the system was allowed to equilibrate for 15 min before measurements of the fluorescence intensity. Slits with a nominal band-pass of 6 nm were used to measure REES upon changing the excitation wavelength. In polarized fluorescence measurements, the excitation beam passed through a polarizer and was then focused by an elliptical mirror onto the air/water interface. To select either the p- or s-polarized component of the monolayer fluorescence, another polarizer was placed before the mirror collecting the emitted light prior to its detection by a CCD camera.<sup>27</sup> These experiments were carried out in a dark room, and electronic shutters were used to irradiate monolayers within 30 s.

(24) Dutta, A. K.; Salesse, C. *Langmuir* **1997**, *13*, 5401.

(25) Maloney, K. M.; Grandbois, M.; Grainger, D. W.; Salesse, C.; Lewis, K. A.; Roberts, M. F. *Biochim. Biophys. Acta* **1995**, *1235*, 395.  
(26) Gallant, J.; Lavoie, H.; Tessier, A.; Munger, G.; Leblanc, R. M.; Salesse, C. *Langmuir* **1998**, *14*, 3954.

(27) Vranken, N.; Van der Auwerter, M.; De Schryver, F. C.; Lavoie, H.; Bélanger, P.; Salesse, C. *Langmuir* **2000**, *16*, 9518.

(18) Demchak, R. J.; Fort, T., Jr. *J. Colloid Interface Sci.* **1974**, *46*, 191.

(19) Petrov, J. G.; Polymeropoulos, E. E.; Möhwald, H. *J. Phys. Chem.* **1996**, *100*, 9860.

(20) Oliveira, O. N., Jr.; Taylor, D. M.; Stirling, C. J. M.; Tripathi, S.; Guo, B. Z. *Langmuir* **1992**, *8*, 1619.

(21) Oliveira, O. N., Jr.; Taylor, D. M.; Lewis, T. J.; Salvagno, S.; Stirling, C. J. M. *J. Chem. Soc., Faraday Trans. 1* **1989**, *85*, 1009.

(22) Ahluwalia, A.; Piolanti, R.; De Rossi, D.; Fissi, A. *Langmuir* **1997**, *13*, 5909.

(23) Oliveira, O. N., Jr.; Bonarsi, C. *Langmuir* **1997**, *13*, 5920.

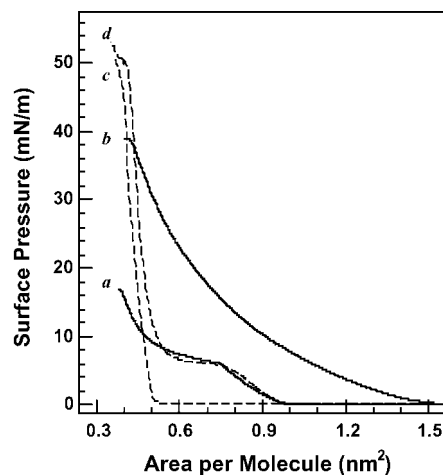


**Figure 2.**  $\pi$ - $A$  isotherms of the DPPE-NBD (a), NBD(C<sub>12</sub>)-PC (b), DPPE (c) and DPPC (d) monolayers at the air/water interface. The isotherms were measured at  $20 \pm 1$  °C and a compression speed of  $0.05 \text{ nm}^2/(\text{molecule} \cdot \text{min})$ .

### 3. Results and Discussion

**3.1. Surface Pressure–Area ( $\pi$ - $A$ ) Isotherms and Morphology of NBD-Phospholipid Monolayers.** The  $\pi$ - $A$  isotherms of the studied phospholipid monolayers on water are presented in Figure 2. Isotherms of the DPPE and DPPC monolayers are essentially the same as those reported earlier,<sup>11,28–30</sup> have already been analyzed in detail in these reports, and are used only as references here.

Comparing the isotherms of parent phospholipids with those of NBD-labeled analogues, the influence of the attachment of the NBD chromophore either to the headgroup or to the aliphatic chain is readily apparent. Significant differences in monolayer behavior of the NBD-phospholipids and the parent phospholipids are observed. Notably, the surface pressure lift-off of the DPPE-NBD isotherm is shifted toward larger molecular areas over that of DPPE. Additionally, the DPPE-NBD isotherm exhibits typical liquid-expanded behavior with monotonically increasing surface pressure in the  $0.96$ – $0.74 \text{ nm}^2/\text{molecule}$  region in contrast to monolayers of DPPE remaining in the condensed state, showing no distinct liquid-expanded states or phase transitions. Significantly, a plateau-like region appears in the isotherm of NBD-labeled DPPE at areas below  $0.74 \text{ nm}^2/\text{molecule}$ , and plateau pressure increased with increasing temperature. Though the isotherms measured at different temperatures were similar in shape, the plateau pressure rose from  $3$  to  $7 \text{ mN/m}$  as subphase temperatures increased from  $10$  to  $20$  °C while the area corresponding to the plateau onset decreased (data not shown). Upon subsequent compression–expansion, very little hysteresis occurred, suggesting that the process leading to the appearance of the plateau is completely reversible. Such behavior is a strong indication that the plateau originates from phase coexistence associated with a first-order phase transition between the liquid-expanded (LE) and liquid-condensed (LC) monolayer states.<sup>31,32</sup> The DPPE-NBD monolayer collapses at an area of  $0.38 \text{ nm}^2/\text{molecule}$  and a surface pressure of

approximately  $17 \text{ mN/m}$  that is surprisingly low compared to that of the parent phospholipid.

Analogously, the onset of the surface pressure for the NBD(C<sub>12</sub>)-PC monolayer is detected at an area of  $1.5 \text{ nm}^2/\text{molecule}$ , which is remarkably larger than the area per molecule corresponding to the surface pressure lift-off of the DPPC isotherm (Figure 2). However, the isotherm of the NBD-labeled analogue of DPPC lacks any of the plateau features typically observed in the isotherm of DPPC at areas between  $0.8$  and  $0.55 \text{ nm}^2/\text{molecule}$ .<sup>11,28–30</sup> The NBD(C<sub>12</sub>)-PC monolayer shows only an LE state and collapses at an area of  $0.43 \text{ nm}^2/\text{molecule}$  and a surface pressure of  $39 \text{ mN/m}$ . Surprisingly, while the attachment of NBD chromophore increases the area per phospholipid molecule in the expanded state by approximately  $0.45 \text{ nm}^2$  for both phospholipids compared to the parent phospholipids, the molecular area in the condensed state does not seem to be affected by the presence of the NBD moiety. A similar observation was made by Huster et al.<sup>6</sup> for NBD-phosphatidylcholine-containing bilayers where the NBD group induced an increase in the average area per phosphatidylcholine molecule of  $0.02 \text{ nm}^2$ , a less than 3% increase in area per molecule over that of the parent phospholipid.

The first-order LE–LC transition for the DPPE-NBD monolayer was visualized directly by epifluorescence microscopy. As shown in Figure 3A, the monolayer was homogeneously fluorescent in the expanded region of the isotherm. Upon further compression to areas below  $0.74 \text{ nm}^2/\text{molecule}$ , phase separation is induced. As clearly seen in Figure 3B, there are two phases, dark condensed domains and fluorescent background, coexisting in the plateau region of the DPPE-NBD isotherm. Small rosette-shaped domain structures appeared initially near the onset of the plateau and, as compression proceeded, grew larger in size. Though the domains coexisting at a given surface pressure differ in size (i.e., from locally different compression conditions and kinetic artifacts), they are relatively homogeneous in shape, making six-petalled rosettes, and distributed evenly over the field. Domains contact each other at a surface pressure of approximately  $17 \text{ mN/m}$ , but they do not appear to coalesce. Instead, further imaging shows the lack of crispness and a progressive blurring of the domain boundaries (data not shown). This effect was previously observed for monolayers of phospholipids mixed with NBD-labeled analogues<sup>13,33</sup> and interpreted as an increased light scattering at multilayered exclusion structures (collapsed phase) containing NBD-phospholipids. Nevertheless, the series of micrographs captured during the compression–expansion run showed that the monolayer respread readily with decreasing surface pressure and the order in which the domains appeared and grew upon compression was completely reversed upon decompression (data not shown). This is in accord with the lack of observable hysteresis in the  $\pi$ - $A$  isotherm of DPPE-NBD, further supporting that the plateau indeed corresponds to a first-order LE–LC phase transition.

More complex morphology was observed for the NBD-(C<sub>12</sub>)-PC monolayer. A uniform fluorescent field was observed in the  $1.5$ – $0.82 \text{ nm}^2/\text{molecule}$  region (Figure 4A). However, upon further decreasing the area per molecule, small domains started to appear. As seen in Figure 4B, these structures varied in both shape and size, representing domains of two kinds irregularly distributed over the field. Tiny dark circular spots and relatively large strongly

(28) Ducharme, D.; Max, J.-J.; Salesse, C.; Leblanc, R. M. *J. Phys. Chem.* **1990**, *94*, 1925.

(29) Vogel, V.; Möbius, D. *J. Colloid Interface Sci.* **1988**, *126*, 408.

(30) Gaub, H. E.; Moy, V. T.; McConnell, H. M. *J. Phys. Chem.* **1986**, *90*, 1721.

(31) Marcelja, S. *Biochim. Biophys. Acta* **1974**, *367*, 165.

(32) Pallas, N. R.; Pethica, B. A. *Langmuir* **1995**, *1*, 509.

(33) Krüger, P.; Schalke, M.; Wang, Z.; Notter, R. H.; Dluhy R. A.; Lösche, M. *Biophys. J.* **1999**, *77*, 903.



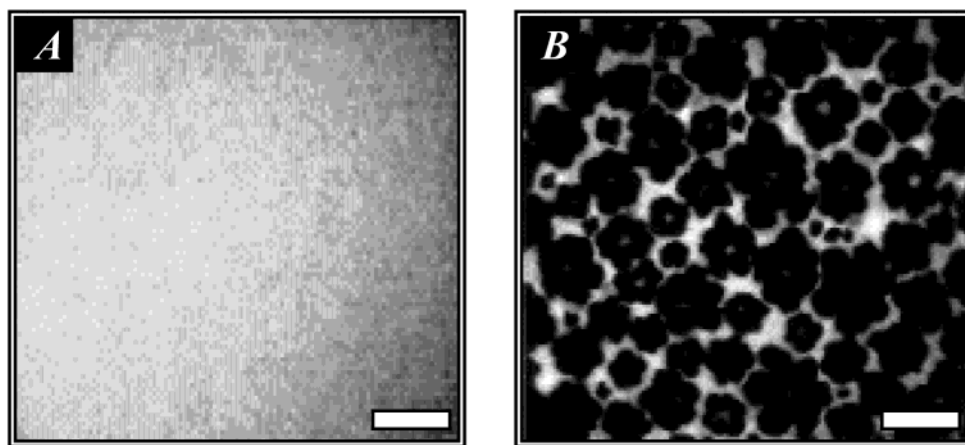


**Figure 3.** Typical epifluorescence micrographs for a DPPE-NBD monolayer in the expanded region (A) and in the plateau (B) of the  $\pi$ - $A$  isotherm. Micrograph B was taken at  $A = 0.55 \text{ nm}^2/\text{molecule}$  and  $\pi = 8 \text{ mN/m}$ . The scale bars are  $40 \text{ }\mu\text{m}$ .

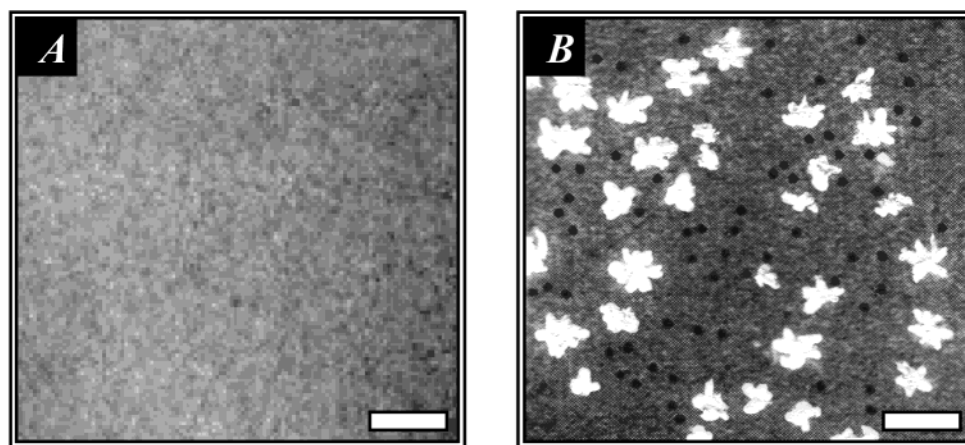


**Figure 4.** Typical epifluorescence micrographs for an NBD(C<sub>12</sub>)-PC monolayer in the  $1.5\text{--}0.82 \text{ nm}^2/\text{molecule}$  region (A) and at areas below  $0.82 \text{ nm}^2/\text{molecule}$  (B). Micrograph B was taken at  $A = 0.5 \text{ nm}^2/\text{molecule}$  and  $\pi = 33 \text{ mN/m}$ . The scale bars are as in Figure 3.

fluorescent domains in a low-intensity fluorescent background were typical of the micrographs taken at areas below  $0.82 \text{ nm}^2/\text{molecule}$ . As compression proceeded, domains of both kinds grew slightly larger in size.

The observation of domains in the micrographs of an LE-type monolayer such as that of NBD(C<sub>12</sub>)-PC (see isotherm b, Figure 2), which is presumed to exhibit a single homogeneous phase up to the point of monolayer collapse, is unexpected. However, even more striking is the fact that replacement of one aliphatic chain in DPPC by an NBD-labeled chain changes the organization of DPPC at the air/water interface in a way that effectively prevents phosphatidylcholine molecules from their well-recognized formation of ferroelectric domains.<sup>12,34</sup> Thus, it is clear that the unique morphology observed for the NBD(C<sub>12</sub>)-PC monolayer as well as the formation of a hexatic phase in the DPPE-NBD monolayer should be considered in terms of localization of NBD chromophores at the interface and their interactions with each other and with the headgroups of phospholipid molecules as discussed below.

**3.2. Surface Potential–Area ( $\Delta V$ - $A$ ) Isotherms and Localization of the NBD Chromophore at the Air/Water Interface.** Since the isotherms of both NBD-labeled phospholipids reach almost the same areas per molecule near monolayer collapse as those of the parent phospholipids, the NBD group might be assumed to be either buried beneath the DPPE-NBD headgroup or

elevated on top of the NBD(C<sub>12</sub>)-PC monolayer to achieve monolayer packing densities similar to those of the parent phospholipids lacking NBD. To assess in a first approximation the orientation of the NBD moiety at the interface, surface potential measurements were performed. The  $\Delta V$ - $A$  isotherms of the NBD-phospholipid and parent phospholipid monolayers at the air/water interface are presented in Figure 5A. Isotherms of the DPPC and DPPE monolayers are similar to those reported elsewhere,<sup>28,29,35</sup> and thus, they are not discussed further, but used for comparison. At large areas per molecule, the surface potential of the NBD(C<sub>12</sub>)-PC monolayer was always positive. As seen in Figure 5A, after the jump, the surface potential rises smoothly and reaches a value of  $+287 \text{ mV}$  at an area of  $0.48 \text{ nm}^2/\text{molecule}$ , slightly larger than the collapse area of the  $\pi$ - $A$  isotherm. In contrast, the DPPE-NBD monolayer exhibits variations of surface potential during compression. No jump in the surface potential is observed on lift-off. The onset of the surface potential is rather difficult to determine, but can be located anywhere between  $1.5$  and  $1.3 \text{ nm}^2/\text{molecule}$ . Then, at an area of approximately  $1.1 \text{ nm}^2/\text{molecule}$ , the surface potential starts to decrease progressively until a minimum value of  $-81 \text{ mV}$  is attained at the beginning of the plateau in the  $\pi$ - $A$  isotherm. Upon further compression, another slope change occurs in the  $\Delta V$ - $A$  isotherm at an area of  $0.83 \text{ nm}^2/\text{molecule}$  from which  $\Delta V$  increases rapidly,

(34) Bowen, P. J.; Lewis, T. J. *Thin Solid Films* **1983**, *99*, 157.

(35) Hayashi, M.; Muramatsu, T.; Hara, I. *Biochim. Biophys. Acta* **1972**, *255*, 98.

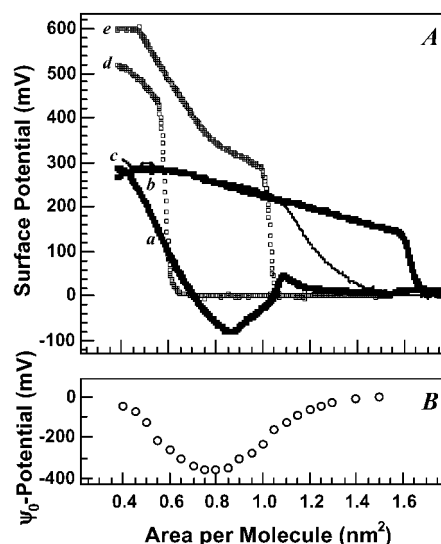


**Figure 5.**  $\Delta V$ - $A$  isotherms of the DPPE-NBD (a) and NBD-(C<sub>12</sub>)-PC (b) monolayers at the air/water interface, DPPE-NBD on an HCl subphase with pH 1.9, DPPE (c), and DPPC (d) (A) and the  $\psi_0$  potential of the DPPE-NBD monolayer (B). The experimental conditions are identical to those in Figure 2.

yielding a value of +291 mV in the fully condensed state. Interestingly, despite the differences in  $\Delta V$ - $A$  isotherms at larger areas per molecule, the values of the surface potentials for both closely packed NBD-phospholipid monolayers were essentially the same. The negative surface potential of the DPPE-NBD monolayer in the expanded region originates probably from the contribution of an electric double layer formed by phosphatidylethanolamine-NBD (PE<sup>-</sup>-NBD) groups and protons, since the monolayer is at least partly ionized at the subphase pH used.<sup>36</sup>

Surface potential,  $\Delta V$ , has been shown to be related to the normal component of group dipole moments of aliphatic molecules forming monolayers at the air/water interface using the Demchak-Fort three-layer capacitor model.<sup>19-23</sup> According to this model, the monolayer surface potential results from the contribution of the dipole moments,  $\mu_i$ , of (1) terminal CH<sub>3</sub> groups, (2) hydrophilic headgroups, and (3) water molecules reoriented and polarized by the monolayer.<sup>18</sup> To take into account the local polarizabilities of the medium surrounding the dipoles, a different effective dielectric constant,  $\epsilon_i$ , is assigned to each layer. In addition, when the monolayer is ionized, an electric double-layer is expected to be formed that contributes to the surface potential,  $\Delta V$ , with the double-layer potential  $\psi_0$ . Applying the Demchak-Fort approach, the surface potential for monolayers of DPPE and DPPE-NBD can be written, respectively, as

$$\Delta V_{\text{DPPE}} = \frac{1}{\epsilon_0 A_{\text{DPPE}}} \left[ 2 \frac{\mu_{\text{CH}_3}}{\epsilon_{\text{CH}_3}} + 2 \frac{\mu_{\text{C=O}}}{\epsilon_{\text{C=O}}} + \frac{\mu_{\text{PE}}}{\epsilon_{\text{PE}}} + \frac{\mu_{\text{H}_2\text{O}}}{\epsilon_{\text{H}_2\text{O}}} \right] + \psi_0 \quad (1)$$

$$\Delta V_{\text{DPPE-NBD}} = \frac{1}{\epsilon_0 A_{\text{DPPE-NBD}}} \left[ 2 \frac{\mu_{\text{CH}_3}}{\epsilon_{\text{CH}_3}} + 2 \frac{\mu_{\text{C=O}}}{\epsilon_{\text{C=O}}} + \frac{\mu_{\text{PE}}}{\epsilon_{\text{PE}}} + \frac{\mu_{\text{NBD}}}{\epsilon_{\text{NBD}}} + \frac{\mu_{\text{H}_2\text{O}}}{\epsilon_{\text{H}_2\text{O}}} \right] + \psi_0 \quad (2)$$

where  $\epsilon_0$  is the permittivity of vacuum,  $A_i$  is the area per molecule,  $\mu_{\text{CH}_3}$ ,  $\mu_{\text{C=O}}$ ,  $\mu_{\text{PE}}$ , and  $\mu_{\text{NBD}}$  are the normal components of the dipole moments of the terminal CH<sub>3</sub> group of the acyl chain, the carbonyl C=O group, the phosphatidylethanolamine headgroup, and the NBD chromophore, respectively. The term  $\mu_{\text{H}_2\text{O}}/\epsilon_{\text{H}_2\text{O}}$  is used to account for the reorientation and polarization of water molecules induced by the phospholipid monolayer. Though the Demchak-Fort model has been widely used to gain microscopic structural or dielectric information,<sup>19-23,37</sup> the model is in some ways tied to questionable assumptions and oversimplifications,<sup>37</sup> as it deals with a number of parameters whose reliable values are difficult, if not impossible, to obtain. In particular, values reported so far for the effective dielectric constant of the terminal CH<sub>3</sub> group region,  $\epsilon_{\text{CH}_3}$ , differ across a range of 2.1–5.3<sup>19,21,37,38</sup> while the  $\mu_{\text{CH}_3}$  value can vary between 0.12 and 0.4 D.<sup>19,29,39</sup> Values for other parameters of eqs 1 and 2 found in the literature differ even more. For instance, depending on the method of analysis, values of  $\mu_{\text{H}_2\text{O}}/\epsilon_{\text{H}_2\text{O}}$  were found within 0.05–10 D,<sup>37,39,40</sup> suggesting that the reorganized water molecules hydrating lipid polar headgroups could contribute from 4 up to 500 mV to the measured  $\Delta V$ . Therefore, the aim of the present analysis of  $\Delta V$  data is to make, on a comparative basis, a rough estimation of the NBD chromophore contribution to the normal component of the phospholipid dipole moment, whether it is negative or positive, rather than to derive any quantitative information.

We argue that the decrease of approximately 230 mV observed in the surface potential of the fully condensed monolayer of DPPE-NBD compared to DPPE is due mainly to the presence of the NBD group. The NBD chromophore has a permanent dipole moment of 11.8 D in its plane.<sup>41</sup> Moreover, substitution of two headgroup protons by NBD alters the charge distribution of the phosphatidylethanolamine dipole so that only the negative charge on the phosphatidyl group remains. Consequently, the DPPE-NBD monolayer should have a negative  $\psi_0$  potential at a subphase pH of 5.6.<sup>36</sup> Presumably, both the NBD dipole with its projection  $\mu_{\text{NBD}}$  on the surface normal and the  $\psi_0$  potential contribute negatively to the surface potential  $\Delta V$ . Although the NBD-induced distortion of charge distribution likely causes a decrease in the dipole moment of the phosphatidylethanolamine headgroup, its effect on  $\Delta V$  is believed to be relatively minor because the normal component  $\mu_{\text{PE}}$  of the phosphatidylethanolamine dipole is oriented more parallel to the interface and does not seem to be a dominant contributor to the surface potential.<sup>18,21,29,36</sup> The presence of the NBD chromophore will also alter the ordering of water molecules in the hydration shell of the phosphatidylethanolamine headgroup<sup>42</sup> and, as a result, may affect, to some extent, the value of  $\mu_{\text{H}_2\text{O}}/\epsilon_{\text{H}_2\text{O}}$ . However, this type of change is expected to increase the value of  $\Delta V$  rather than decrease it. As mentioned above, though a lot of controversy over the contribution of ordered water dipoles to  $\Delta V$  exists, the value is estimated to be approximately +93 and +124 mV for phosphatidylethanolamine and phosphatidylcholine monolayers, respectively.<sup>37,40</sup> A more positive contribution of ordered water dipoles to  $\Delta V$  of phosphatidylcholine can be attributed to the progressive increase in hydration level as

(37) Brockman, H. *Chem. Phys. Lipids* **1994**, 73, 57.

(38) Taylor, D. M.; Bayes, G. F. *Phys. Rev. E* **1994**, 49, 1439.

(39) Raudino, A.; Mauzerall, D. *Biophys. J.* **1986**, 50, 441.

(40) Gawrisch, K.; Ruston, D.; Zimmerberg, J.; Parsegian, V. A.; Rang, R. P.; Fuller, N. *Biophys. J.* **1992**, 61, 1213.

(41) Müller, P.; Gallet, F. *J. Phys. Chem.* **1991**, 95, 3257.

(42) Willard, D. M.; Riter, R. E.; Levinger, N. E. *J. Am. Chem. Soc.* **1998**, 120, 4151.

(36) Tocanne, J.-F.; Teissie J. *Biochim. Biophys. Acta* **1990**, 1031, 111.

one goes from phosphatidylethanolamine to phosphatidylcholine through the addition of methyl groups: the former phospholipid was found to bind 7–12 water molecules, while values ranging from 30 to 35 water molecules per phospholipid were reported for the latter.<sup>43</sup> Due to the presence of the NBD chromophore, a larger headgroup size will likely favor a further increase in hydration. Nevertheless, comparing the hydration potentials of phosphatidylethanolamine and phosphatidylcholine, large changes in hydration give rise to a value of  $\mu_{\text{H}_2\text{O}}/\epsilon_{\text{H}_2\text{O}}$  equivalent to an increase in  $\Delta V$  of  $\sim 31$  mV. Hence, considering that this simplification leads to some underestimation of group dipole contributions, we choose to neglect changes in  $\mu_{\text{H}_2\text{O}}/\epsilon_{\text{H}_2\text{O}}$  due to NBD incorporation in the phospholipid structure in our calculations as relatively insignificant. Then, we will consider that for a given temperature, pH and area per molecule the contributions of  $\mu_{\text{CH}_3}/\epsilon_{\text{CH}_3}$  and of  $\mu_{\text{C=O}}/\epsilon_{\text{C=O}}$  to  $\Delta V$  are identical to those pertaining to the DPPE monolayer.<sup>20</sup> Thus, we may ascribe differences in the surface potentials of DPPE and DPPE-NBD mainly to the substitution of two phosphatidylethanolamine headgroup protons by the NBD chromophore. Then, we may write, after the subtraction of eq 1 from eq 2

$$\mu_{\text{NBD}}/\epsilon_{\text{NBD}} = \epsilon_0 A (\Delta V_{\text{DPPE-NBD}} - \psi_0 - \Delta V_{\text{DPPE}}) \quad (3)$$

where  $\psi_0$  is the double-layer potential of the DPPE-NBD monolayer. On the basis of the intrinsic  $\text{p}K_a$  of the phosphatidylethanolamine headgroup, DPPE can be considered as a zwitterion bearing a permanent positive charge on the amine group and a negative charge on the phosphatidyl group over a pH range of 2.3–8.<sup>36</sup> As a result, the contribution of the  $\psi_0$  potential in  $\Delta V_{\text{DPPE}}$ , in particular, at pH 5.6 will be negligible.

To calculate  $\mu_{\text{NBD}}/\epsilon_{\text{NBD}}$  using eq 3, the  $\psi_0$  potential of the DPPE-NBD monolayer should be determined. As suggested by Dynarowicz-Latka et al.,<sup>44</sup> a portion of  $\Delta V$  associated with the double-layer potential can be found through a comparison of the surface potentials of a nonionized DPPE-NBD monolayer on an acidic subphase and an ionized one on pure water. Given an intrinsic  $\text{p}K_a$  of 0.32–0.7 for the phosphatidyl group<sup>36</sup> and taking into account the ionization properties of the NBD chromophore,<sup>1,10</sup> it is reasonable to expect that the  $\text{PE}^-$ -NBD group will be completely neutralized by a proton, probably in the form of an ion pair, at a subphase pH  $\leq 2$ . Thus, to obtain the dependence of the  $\psi_0$  potential on the area per molecule for the DPPE-NBD monolayer on pure water, the  $\Delta V$ - $A$  isotherm of the DPPE-NBD monolayer spread onto a subphase containing HCl at a pH of 1.9 was measured (curve c in Figure 5) and, then, subtracted from the  $\Delta V$ - $A$  isotherm shown in Figure 5A (curve a). The dependence of the  $\psi_0$  potential on the area per molecule is presented in Figure 5B. The fact that the resulting  $\psi_0$  potential does not obey the exponential dependence predicted by the Gouy–Chapman model is worth special attention and will be discussed below. Since values of the  $\psi_0$  potential of the DPPE-NBD monolayer at the air/water interface at different areas per molecule can be obtained from Figure 5B, the value of  $\mu_{\text{NBD}}/\epsilon_{\text{NBD}}$  can be readily assessed using eq 3. In the 0.6–0.4 nm<sup>2</sup>/molecule region, eq 3 yields  $\mu_{\text{NBD}}/\epsilon_{\text{NBD}} \approx -0.23$  D (to convert the calculated value of  $\mu_{\text{NBD}}/\epsilon_{\text{NBD}}$  into Debye units, the conversion factor 1 D =  $3.335 \times 10^{-30}$  C·m was applied<sup>29</sup>). We stress that, although the absolute value of  $\mu_{\text{NBD}}/\epsilon_{\text{NBD}}$  might be underestimated due to the simplification of our analysis,

the contribution of  $\mu_{\text{NBD}}/\epsilon_{\text{NBD}}$  to  $\Delta V$  was indeed found to be negative, which is not unreasonable as explained below.

The NBD heterocyclic chromophore is flat and, because of the distribution of charges in its structure, bears a permanent electric dipole moment oriented as drawn schematically in Figure 6a, making an angle of 43° with respect to the N–NO<sub>2</sub> axis.<sup>41</sup> With this model, it is thus possible to discuss the orientation of the dipole moment  $M$  at the air/water interface on the basis of the  $\Delta V$  data analysis. Recent calculations<sup>29,36</sup> showed that a positive portion of  $\Delta V$  of the DPPE monolayer originates from two main dipole moments:  $\mu_{\text{CH}_3}$  that characterizes the aliphatic chain terminal group and  $\mu_{\text{C=O}}$  corresponding to the carbonyl C=O group of the phospholipid molecule. Structural studies on phospholipid monolayers and bilayers<sup>36</sup> indicated that both dipoles in a closely packed state were oriented essentially parallel to the surface normal with their strong projected dipole moments  $\mu_{\text{CH}_3}$  and  $\mu_{\text{C=O}}$  directed into the monolayer (see Figure 6b), thus contributing positively to the surface potential. By contrast, the phosphatidylethanolamine dipole with its ethanolamine group slightly repelled away from the monolayer toward the water subphase gives the projection  $\mu_{\text{PE}}$  onto the surface normal antiparallel to  $\mu_{\text{CH}_3}$  and  $\mu_{\text{C=O}}$  as shown in Figure 6b. As a result, it contributes negatively to the surface potential.<sup>29,36</sup> Consequently, the negative  $\mu_{\text{NBD}}/\epsilon_{\text{NBD}}$  value implies that the orientation of the NBD dipole moment  $M$  at the air/water interface must be similar to that of the phosphatidylethanolamine dipole. Therefore, any orientation of the NBD group as shown in Figure 6c may be ascribed to the NBD chromophore in the DPPE-NBD monolayer as long as the projection  $\mu_{\text{NBD}}$  on the surface normal remains negative. As shown in Figure 6b, the depiction with the NBD chromophore located underneath the phosphatidylethanolamine group is consistent with the conclusion derived from the  $\pi$ - $A$  isotherm: the NBD group does not require any additional area in the condensed monolayer. Indeed, given the size of the NBD group (approximately 0.6 nm  $\times$  0.5 nm in the plane and 0.025 nm thick<sup>45</sup>), such a localization (Figure 6b) will not alter the area per molecule in the condensed state to any remarkable extent because the area of  $\sim 0.125$  nm<sup>2</sup> required per NBD is sufficiently small to be readily accommodated underneath the phosphatidylethanolamine headgroup.

Following a similar approach, the contribution of the NBD chromophore to the surface potential of the NBD-(C<sub>12</sub>)-PC monolayer was also estimated. Comparing the  $\Delta V$ - $A$  isotherm of the NBD(C<sub>12</sub>)-PC monolayer (curve b, Figure 5A) and that of the parent phospholipid (curve d, Figure 5A), the attachment of the NBD chromophore terminally to an aliphatic chain notably causes a decrease in  $\Delta V$  of 320 mV. As the headgroup of both monolayer-forming compounds is phosphatidylcholine completely ionized at pH 5.6 used in the experiments, the presence of both DPPC and NBD(C<sub>12</sub>)-PC at the interface in zwitterionic form rules out the possibility for the double-layer  $\psi_0$  potential to alter the monolayer  $\Delta V$ . Moreover, both monolayers collapse at approximately the same area per molecule, so that at the end of the isotherm the terminal CH<sub>3</sub> group, the carbonyl, and the phosphatidylcholine dipole moments of the DPPC and NBD(C<sub>12</sub>)-PC molecules are probably all projected alike onto the surface normal. Consequently, the contributions  $\mu_{\text{CH}_3}/\epsilon_{\text{CH}_3}$ ,  $\mu_{\text{C=O}}/\epsilon_{\text{C=O}}$  and  $\mu_{\text{PC}}/\epsilon_{\text{PC}}$  as well as the contribution of the oriented water dipoles,  $\mu_{\text{H}_2\text{O}}/\epsilon_{\text{H}_2\text{O}}$ , to  $\Delta V$  of both monolayers are almost identical at a given temperature, pH, and area per molecule.<sup>20</sup> Then, the decrease in  $\Delta V_{\text{NBD(C}_{12}\text{)}-\text{PC}}$  com-

(43) Sen, A.; Hui, S.-W. *Chem. Phys. Lipids* **1988**, *49*, 179.

(44) Dynarowicz-Latka, P.; Dhanabalan, A.; Cavalli, A.; Oliveira, O. N., Jr. *J. Phys. Chem. B* **2000**, *104*, 1701.

(45) Flament, C.; Graf, K.; Gallet, F.; Riegler, H. *Thin Solid Films* **1994**, *243*, 411.



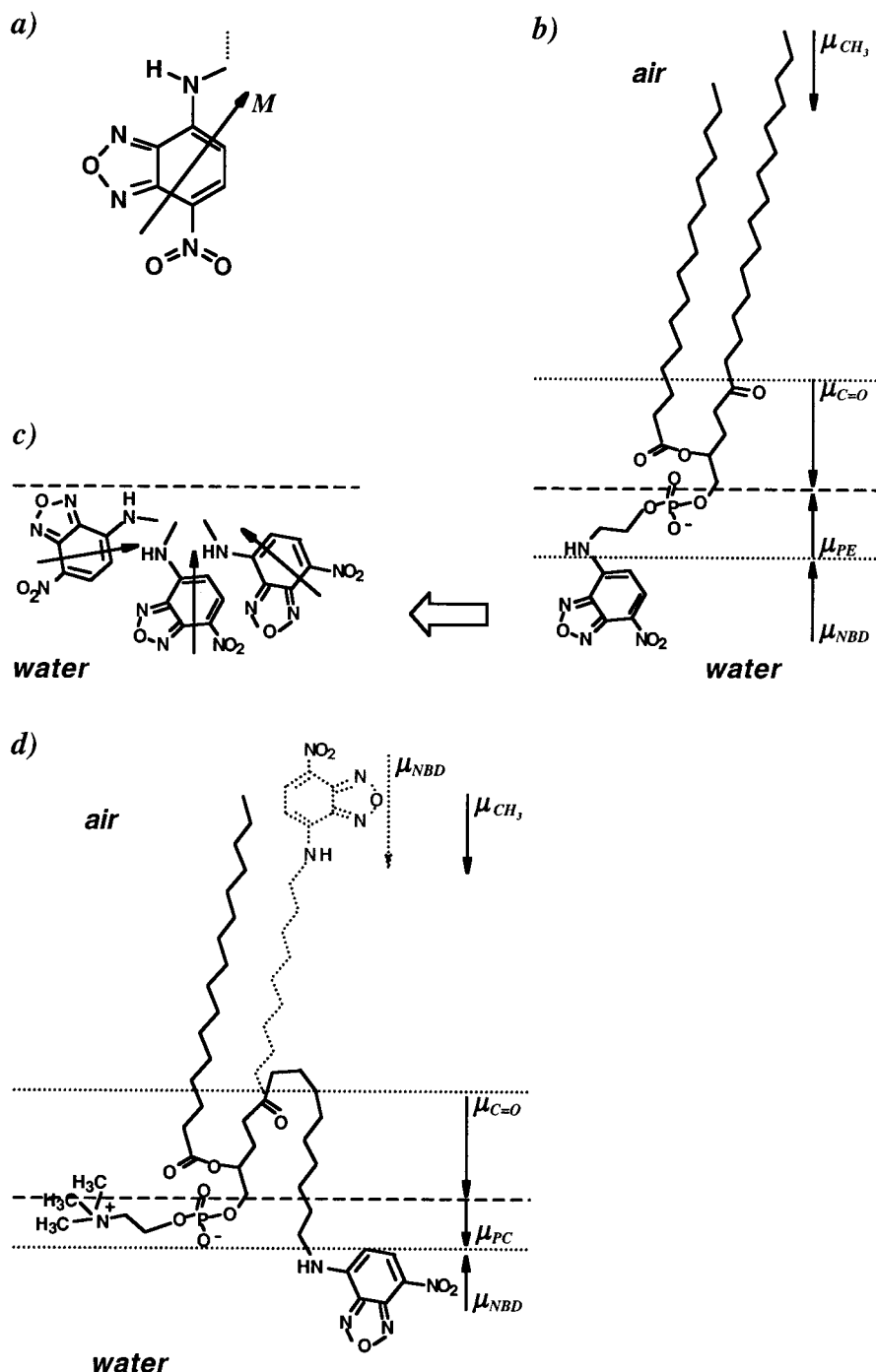


**Figure 6.** Schematic depiction of the structure of the NBD chromophore and its orientation at the air/water interface. (a) A permanent dipole moment,  $M$ , in the NBD group. The drawing is made on the basis of previously reported data.<sup>39,43,44</sup> (b) A schematic diagram of the DPPE-NBD molecule orientation at the air/water interface.  $\mu_{CH_3}$  and  $\mu_{C=O}$  are the normal components of the dipole moments of aliphatic chain termini and carbonyl groups of the molecule, respectively. By being directed into the monolayer, they contribute positively to  $\Delta V$ .<sup>34</sup>  $\mu_{PE}$  and  $\mu_{NBD}$  are the normal components of the phosphatidylethanolamine dipole and NBD dipole, respectively. By being antiparallel to  $\mu_{CH_3}$  and  $\mu_{C=O}$ , they provide a negative contribution to  $\Delta V$ .<sup>27,34</sup> (c) NBD orientations corresponding to negative projection  $\mu_{NBD}$ . (d) A schematic diagram of the NBD(C12)-PC molecule orientation at the air/water interface. The normal components  $\mu_{CH_3}$ ,  $\mu_{C=O}$ , and  $\mu_{NBD}$  are as in drawing b, while  $\mu_{PC}$  is the normal component of the P<sup>-</sup>-N<sup>+</sup> phosphatidylcholine dipole. The dotted drawing shows the orientation of the NBD-labeled chain which could result in a positive contribution of  $\mu_{NBD}$  to  $\Delta V$ . A negative contribution of  $\mu_{NBD}$  to  $\Delta V_{NBD(C12)-PC}$  suggests looping of the NBD-labeled acyl chain toward water. A detailed explanation is given in the text. Drawings b and d are made on the basis of previously reported models.<sup>27,34</sup>

pared to  $\Delta V_{DPPC}$  likely arises from the substitution of one chain terminal  $CH_3$  group by the NBD moiety, given by

$$\Delta V_{NBD(C12)-PC} - \Delta V_{DPPC} = \frac{1}{\epsilon_0 A} \left( \frac{\mu_{NBD}}{\epsilon_{NBD}} - \frac{\mu_{CH_3}}{\epsilon_{CH_3}} \right) \quad (4)$$

Solving eq 4 for  $\mu_{NBD}/\epsilon_{NBD}$ , we may write

$$\frac{\mu_{NBD}}{\epsilon_{NBD}} = \frac{\epsilon_0 A (\Delta V_{NBD(C12)-PC} - \Delta V_{DPPC})}{3.335 \times 10^{-30}} + \frac{\mu_{CH_3}}{\epsilon_{CH_3}} \quad (5)$$

The value of  $\mu_{CH_3}/\epsilon_{CH_3}$  for a chain terminal group has been determined previously from a comparative analysis of the  $\pi$ - $A$  and  $\Delta V$ - $A$  isotherms of stearic acid and a 1:1 mixture of octadecane and octadecylmalonic acid. In this study,

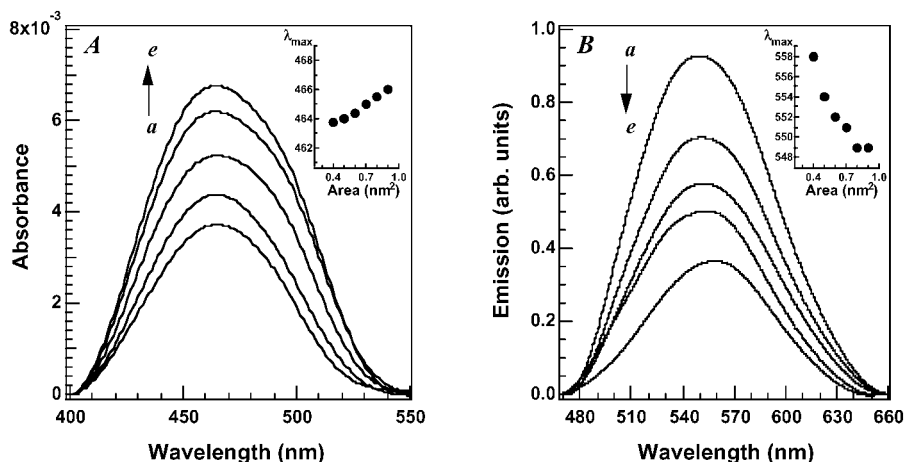


**Figure 7.** Corrected absorption (A) and emission (B) spectra of the DPPE-NBD monolayer at the air/water interface recorded in different regions of the  $\pi$ -A isotherm: (a)  $A = 0.9$  nm<sup>2</sup>/molecule,  $\pi = 1.9$  mN/m; (b)  $A = 0.7$  nm<sup>2</sup>/molecule,  $\pi = 6.4$  mN/m; (c)  $A = 0.6$  nm<sup>2</sup>/molecule,  $\pi = 7.8$  mN/m; (d)  $A = 0.5$  nm<sup>2</sup>/molecule,  $\pi = 9.2$  mN/m; (e)  $A = 0.4$  nm<sup>2</sup>/molecule,  $\pi = 15.8$  mN/m. The emission spectra were obtained using an excitation wavelength of 465 nm. The inset shows the dependence of the absorption (emission) maximum,  $\lambda_{\max}$ , on the area per molecule.

Vogel and Möbius derived  $\mu_{\text{CH}_3}/\epsilon_{\text{CH}_3} \approx +0.35$  D.<sup>29</sup> Applying this value, we calculate a value of  $-0.05$  D for  $\mu_{\text{NBD}}/\epsilon_{\text{NBD}}$  in the  $0.55$ – $0.4$  nm<sup>2</sup>/molecule region. In fact, this value of  $-0.05$  D is surprisingly small for the NBD chromophore possessing a permanent dipole moment of  $11.8$  D. Such a negative contribution of the NBD dipole to the surface potential of the NBD(C<sub>12</sub>)-PC monolayer is somewhat unexpected. Assuming an upright orientation of the NBD-labeled chain, it would be reasonable to expect the NBD chromophore to be oriented as shown by the dotted drawing in Figure 6d. However, if the NBD dipole were indeed oriented in this way, it would contribute positively to  $\Delta V$  in analogy to the CH<sub>3</sub> and C=O dipoles discussed above. This does not agree with the value calculated for  $\mu_{\text{NBD}}/\epsilon_{\text{NBD}}$ . In fact, the negative  $\mu_{\text{NBD}}/\epsilon_{\text{NBD}}$  value implies that the NBD chromophore orientation in the NBD(C<sub>12</sub>)-PC monolayer must be similar to that in the DPPE-NBD monolayer (Figure 6b,c). A plausible explanation exists if the chain bearing the NBD moiety loops toward water, leading to localization of the NBD group in the vicinity of the phosphatidylcholine headgroup as drawn schematically in Figure 6d. The same conclusion was made previously for NBD(C<sub>12</sub>)-PC incorporated into lipid bilayers and membranes.<sup>1,3,6,10</sup> Such "looping" of the NBD-labeled acyl chain in the NBD(C<sub>12</sub>)-PC monolayer proposed from the negative  $\mu_{\text{NBD}}/\epsilon_{\text{NBD}}$  value is further supported by the absorption and fluorescence spectroscopy data.

**3.3. Absorption and Fluorescence Spectroscopy of NBD-Phospholipid Monolayers.** An important feature of the NBD chromophore photophysical behavior is the charge transfer (CT) between the electron-donating amino group and the electron-accepting nitro group, which varies with the polarity of the environment surrounding the chromophore.<sup>1,3,7,42,45–47</sup> The CT band of NBD undergoes a significant red shift with increasing polarity and can be utilized to evaluate the chromophore localization at the interface.<sup>1,10</sup> In particular, when the NBD group is placed in nonpolar hydrocarbon solvents, the absorption maximum occurs between  $420$  and  $450$  nm, while in a polar medium, such as protic solvents or water, maximum absorption wavelengths of the CT band cover a narrow range near  $470$  nm.<sup>3,7,46,47</sup> The nature of the environment has an even larger effect on the position of the NBD

fluorescence maximum. Chattopadhyay et al.<sup>10</sup> and Fery-Fergues et al.<sup>10</sup> found that, as the dielectric constant increased, the NBD emission maximum shifted significantly from  $491$ – $519$  nm in hydrocarbon solvents to  $566$ – $571$  nm in water. Therefore, the position of the absorption and fluorescence maxima should provide a rough indication of the polarity of the environment locally around the NBD group.

The DPPE-NBD monolayer absorption and fluorescence spectra recorded at different areas per molecule are presented in Figure 7. Absorption spectra in Figure 7A exhibit a maximum at approximately  $466$  nm that undergoes a small blue shift with decreasing area per molecule as shown in the inset of this figure. The fluorescence emission maxima (Figure 7B) occur over wavelength ranges near  $549$  nm at large molecular areas. As seen in the inset of Figure 7B, a progressive red shift of the fluorescence maximum was observed at areas below the onset of the plateau in the  $\pi$ -A isotherm. The fluorescence intensity decreased continuously upon compression, very consistent with the growth of the nonfluorescent domains in the DPPE-NBD monolayer displayed by the micrograph in Figure 3B. Thus, in comparison with the behavior of NBD in solutions of varying polarity discussed above, the positions of the absorption and fluorescence maxima at  $466$  and  $549$  nm, respectively, indicate that the NBD group of the DPPE-NBD molecule is located in the polar environment of the monolayer headgroup region.

As seen in Figure 8, the absorption and fluorescence spectra of the NBD(C<sub>12</sub>)-PC monolayer appear at even longer wavelengths than those of the DPPE-NBD monolayer. Indeed, the absorption maximum of the NBD chromophore in the liquid-expanded NBD(C<sub>12</sub>)-PC monolayer was detected at  $478$  nm (Figure 8A), while its fluorescence maximum was located at approximately  $558$  nm (Figure 8B). Upon further compression, a very small red shift of the absorption band was observed. The emission maximum was also shifted to the red as shown in the Figure 8B inset, and the fluorescence intensity increased significantly at areas below  $0.82$  nm<sup>2</sup>/molecule. The latter effect is probably associated with formation of highly fluorescent domains in the NBD(C<sub>12</sub>)-PC monolayer seen in Figure 4B. Since the positions of both absorption and fluorescence maxima in Figure 8 are very close to the values of  $482$  and  $566$  nm reported by Fery-Fergues et

(46) Fery-Forgues, S.; Fayet, J.-P.; Lopez, A. *J. Photochem. Photobiol. A* **1993**, *70*, 229.

(47) Mukherjee, S.; Chattopadhyay, A.; Samanta, A.; Soujanya, T. *J. Phys. Chem.* **1994**, *98*, 2809.



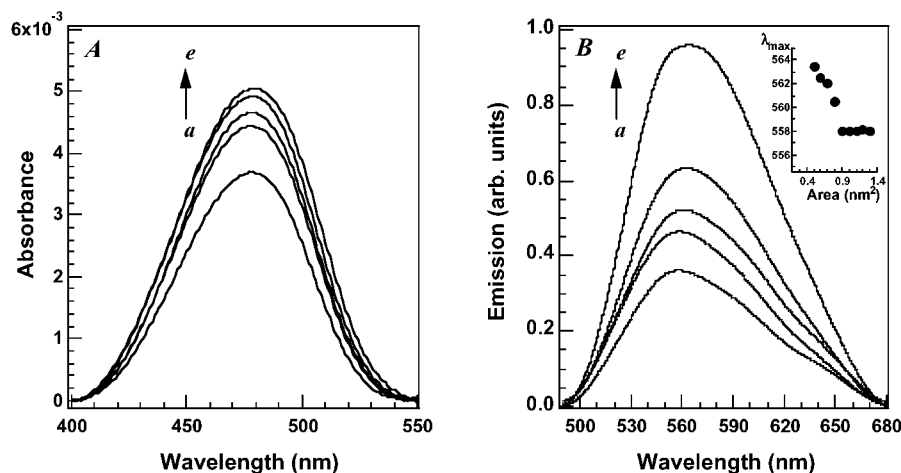


**Figure 8.** Corrected absorption (A) and emission (B) spectra of the NBD(C<sub>12</sub>)-PC monolayer at the air/water interface recorded in different regions of the  $\pi$ - $A$  isotherm: (a)  $A = 1.3 \text{ nm}^2/\text{molecule}$ ,  $\pi = 2.1 \text{ mN/m}$ ; (b)  $A = 0.9 \text{ nm}^2/\text{molecule}$ ,  $\pi = 9.8 \text{ mN/m}$ ; (c)  $A = 0.7 \text{ nm}^2/\text{molecule}$ ,  $\pi = 16.2 \text{ mN/m}$ ; (d)  $A = 0.6 \text{ nm}^2/\text{molecule}$ ,  $\pi = 22.1 \text{ mN/m}$ ; (e)  $A = 0.5 \text{ nm}^2/\text{molecule}$ ,  $\pi = 33 \text{ mN/m}$ . The emission spectra were obtained using an excitation wavelength of 470 nm. The inset shows the dependence of the emission maximum,  $\lambda_{\text{max}}$ , on the area per molecule.

al.<sup>46</sup> for the absorption and fluorescence maxima of the CT band of NBD in water, our absorption and fluorescence data clearly argue in favor of a strongly polar environment surrounding the NBD group in the NBD-DPPC monolayer. Additionally, the fluorescence emission maximum of the NBD chromophore residing in nonpolar regions of an NBD-cholesterol-containing membrane<sup>10</sup> and an NBD-ubiquinone vesicle<sup>49</sup> was reported to be at 522–527 nm, wavelengths shorter than the emission maximum in our experiments. We then conclude that the NBD group of NBD(C<sub>12</sub>)-PC is likely expelled from the monolayer hydrocarbon chain region toward the water subphase and is exposed to the polar environment of the phosphatidylcholine headgroup region at the air/water interface. In summary, our spectroscopic data are in good agreement with the hypothesis of the looping of the NBD-labeled acyl chain of NBD(C<sub>12</sub>)-PC toward water on the basis of the  $\Delta V$  data analysis. Moreover, this conclusion is further supported by fluorescence quenching experiments performed with the aqueous quencher Cu<sup>2+</sup> described below.

The paramagnetic cupric ion is known to be an efficient soluble quencher of fluorescence of NBD chromophores located near the aqueous phase.<sup>1,49</sup> Cu<sup>2+</sup> quenching is assumed to occur by a dynamic mechanism with an efficiency dependent on the quencher concentration, the degree of quencher binding to the phosphatidylcholine headgroup, and electrostatic interactions between the quencher and phospholipid headgroups.<sup>7,48,49</sup> Injection of Cu<sup>2+</sup> under NBD(C<sub>12</sub>)-PC monolayers typically resulted in a quenching of 28–35% of the NBD fluorescence, suggesting that some population of NBD chromophores attached to the aliphatic chain of NBD(C<sub>12</sub>)-PC is readily accessible to Cu<sup>2+</sup> quencher. This is in good accord with the previously reported data for NBD-phospholipid-containing vesicles<sup>10,49</sup> where direct exposure of NBD groups to aqueous quenchers Cu<sup>2+</sup> and Co<sup>2+</sup> caused a 20–50% decrease in the NBD fluorescence. As the positive  $\Delta V_{\text{NBD(C}_{12}\text{)}-\text{PC}}$  is the origin of an energy barrier against the transport of positively charged species across the monolayer,<sup>36</sup> the Cu<sup>2+</sup> quenching means that at least a portion of the NBD groups are located in a monolayer region where they are exposed directly to the aqueous phase. However,

a more precise interpretation of the Cu<sup>2+</sup> quenching results does not seem possible because the Cu<sup>2+</sup> quenching process may be affected by specific adsorption of Cu<sup>2+</sup> to the phosphatidylcholine group,<sup>4,5,10,49</sup> causing a positive double-layer potential of the monolayer. As a result, cupric ion concentrations near the NBD chromophore are reduced over that in the bulk aqueous phase, and the quencher–chromophore collisions likely occur mainly by lateral diffusion of Cu<sup>2+</sup> bound to the phosphatidylcholine headgroup, leading to a lower quenching efficiency.<sup>4</sup> Nevertheless, observed Cu<sup>2+</sup> quenching indicates that, despite differences in the chemical structure of the studied NBD-phospholipids, a substantial amount of NBD groups from NBD(C<sub>12</sub>)-PC are embedded in the monolayer polar region.

**3.4. Polarized Fluorescence and REES Studies on NBD-Phospholipid Monolayers.** Though the NBD group of DPPE-NBD and that of NBD(C<sub>12</sub>)-PC are proposed to be localized in similar monolayer regions, the different contributions of  $\mu_{\text{NBD}}$  in  $\Delta V_{\text{DPPE-NBD}}$  and  $\Delta V_{\text{NBD(C}_{12}\text{)}-\text{PC}}$  imply that the orientation of the NBD chromophore and structural ordering of NBD-phospholipid molecules are rather different in the DPPE-NBD and NBD(C<sub>12</sub>)-PC monolayers. More information relevant to the organization of NBD-phospholipids in a monolayer can be gained from polarized fluorescence measurements and REES study. As the emission from chromophores uniformly oriented with respect to the direction of the polarized excitation is polarized, measurement of fluorescence polarization or anisotropy provides the average orientation of the emitting chromophore. In particular, the relationship between the fluorescence anisotropy  $r$  and the angle  $\theta$  of the emission dipole away from the surface normal is given by<sup>50</sup>

$$r = \frac{3 \cos^2 \theta - 1}{2} \quad (6)$$

The polarization anisotropy is defined by

$$r = \frac{I_{\text{pp}} - GI_{\text{ps}}}{I_{\text{pp}} + 2GI_{\text{ps}}} \quad (7)$$

where  $I_{\text{pp}}$  and  $I_{\text{ps}}$  are vertically polarized (p-polarized) excitation intensities of the fluorescence emission polar-

(48) Peterson, N. O. *Can. J. Chem.* **1985**, *63*, 77.

(49) Rajarathnam, K.; Hochman, J.; Schindler, M.; Ferguson-Miller, S. *Biochemistry* **1989**, *28*, 3168.

(50) Lakowicz, J. R. *Principles of Fluorescence Spectroscopy*; Plenum Press: New York, 1986.

**Table 1. Fluorescence Anisotropy,  $r$ ,<sup>a</sup> and REES Effect Values<sup>b</sup> for DPPE-NBD and NBD(C<sub>12</sub>)-PC in Monolayers at Different Molecular Areas**

area (nm <sup>2</sup> / molecule)	$r_{\text{DPPE-NBD}}$	$r_{\text{NBD(C}_{12}\text{)-PC}}$	REES <sub>DPPE-NBD</sub> (nm)	REES <sub>NBD(C<sub>12</sub>)-PC</sub> (nm)
0.9	0.22	0.003		
0.7	0.25	0.003	4	
0.6	0.23	0.003	6	2
0.5	0.26	0.003	9	6
0.4	0.27	0.003	14	

<sup>a</sup> Polarized fluorescence was measured using excitation wavelengths of 465 and 470 nm for DPPE-NBD and NBD(C<sub>12</sub>)-PC, respectively. <sup>b</sup> REES values given in the table correspond to the shift of the emission maximum of DPPE-NBD (NBD(C<sub>12</sub>)-PC) upon changing the excitation wavelength from 465 nm (470 nm) to 500 nm.

ized vertically and horizontally (s-polarized), respectively.  $G$  is the grating correction factor, which is the ratio of the sensitivities of the detection system for vertically and horizontally polarized light given by  $G = I_{\text{sp}}/I_{\text{ss}}$ .<sup>2,50</sup> For completely polarized emission  $r = 1$ .<sup>50</sup> However, a value of  $r$  equal to unity is never found for the chromophores either in vitrified solution or at interfaces because of a distribution of chromophore orientations always present between  $\theta$  and  $d\theta$ . Regarding the  $\theta$  distribution, a maximum value of 0.4 should be expected for  $r$  when the absorption and emission dipoles are collinear, and when no processes result in depolarization.<sup>50</sup>

To calculate fluorescence anisotropy,  $r$ , polarized fluorescence spectra from the DPPE-NBD monolayer were measured at different areas per molecule. The values of  $r_{\text{DPPE-NBD}}$  are presented in Table 1: anisotropy of the DPPE-NBD fluorescence remains essentially the same, varying between 0.22 and 0.27 with decreasing area per molecule. This suggests that the NBD chromophore of DPPE-NBD adopts a rather narrow distribution of orientations at the air/water interface characterized by the angle  $\theta$  that remains almost unchanged during monolayer compression. As roughly estimated using eq 6, anisotropy values of 0.22–0.27 correspond to an angle  $\theta$  of 44–46°. In contrast, almost no anisotropy was observed in the fluorescence of the NBD(C<sub>12</sub>)-PC monolayer. Regardless of the combination of excitation and emission polarizations, both  $I_{\text{pp}}$  and  $I_{\text{ps}}$  were roughly constant. As a result, eq 7 yielded a value of 0.003 for  $r_{\text{NBD(C}_{12}\text{)-PC}}$  over the range of areas per molecule listed in Table 1. The possible causes for the complete loss of anisotropy could be that (1) chromophores are all oriented alike, making an angle of 54.7° away from the surface normal, or, on the contrary, (2) the NBD chromophore of NBD(C<sub>12</sub>)-PC does not have a unique orientation at the air/water interface and more than one population of NBD characterized by different angles  $\theta$ <sup>50</sup> exists in the NBD(C<sub>12</sub>)-PC monolayer. It could also be that depolarization associated with either in-plane or out-of-plane chromophore rotational motion occurs during the course of excitation.<sup>2,46,50</sup> To identify whether any of the above explanations is correct, REES measurements were performed for both NBD-phospholipid monolayers.

The fluorescence emission spectra of the DPPE-NBD monolayer presented in Figure 7 were obtained using an excitation wavelength of 465 nm. With excitation at 465 nm the emission maximum occurs within a range of 549–558 nm. Changing the excitation wavelength from 465 to 490 and 500 nm caused a progressive red shift in the emission maximum of DPPE-NBD. Such a dependence of the emission spectra on the excitation wavelength is characteristic of the REES effect. Values of REES for the

DPPE-NBD monolayer at different areas per molecule are listed in Table 1: an REES of 4 nm was observed initially at an area of  $\sim 0.7$  nm<sup>2</sup>/molecule corresponding to the onset of the plateau of the DPPE-NBD isotherm. Then, as compression proceeded, the REES value increased gradually and reached a maximum at an area of 0.4 nm<sup>2</sup>/molecule where a change in the excitation wavelength from 465 to 500 nm resulted in a shift of the emission band from 558 to 572 nm, equivalent to an REES of 14 nm. This observation indicates that the NBD chromophore of DPPE-NBD is in a surrounding matrix where its mobility as well as the reorientational motion of the water dipoles around the excited-state chromophore is considerably restricted.<sup>2</sup>

When compressed to an area of 0.6–0.5 nm<sup>2</sup>/molecule, the NBD(C<sub>12</sub>)-PC monolayer also exhibited an REES. However, the effect of excitation at the red edge of the absorption spectrum on the position of the emission maximum was less pronounced. Indeed, upon changing the excitation wavelength from 470 nm, normally used to obtain the fluorescence spectra in Figure 8, to 500 nm, an REES of the emission band of 6 nm was observed only for the NBD(C<sub>12</sub>)-PC monolayer compressed to an area of 0.5 nm<sup>2</sup>/molecule. The REES of 2–6 nm (Table 1) detected at the end of the  $\pi$ - $A$  isotherm suggests that for a large range of molecular areas the immediate environment of the NBD chromophore of NBD(C<sub>12</sub>)-PC is the aqueous phase adjacent to the headgroup region where the relaxation of water molecules is extremely fast.<sup>2</sup> This explains why no REES effect was observed at areas above 0.6 nm<sup>2</sup>/molecule. These findings are in good accord with the polarized fluorescence measurements and provide further evidence that looping of the NBD-labeled acyl chain projects the NBD group of NBD(C<sub>12</sub>)-PC deeper into the water subphase where the rotation motions of the chromophore and surrounding water dipoles are not restricted to any significant extent by steric hindrance. In contrast, DPPE-NBD molecules are organized in condensed structures represented by the nonfluorescent rosette-shaped domains seen in Figure 3B in which the inherent photophysical properties of NBD are altered by interactions of chromophores with one another and/or with phospholipid headgroups.

**3.5. Structural Ordering of the NBD-Phospholipids in Monolayers.** As mentioned in section 3.2 above, an interesting feature of the DPPE-NBD monolayer behavior is the double-layer  $\psi_0$  potential whose dependence on the area per molecule deviates significantly from that predicted by the Gouy–Chapman theory. Instead of continuous growth of its negative value with increasing surface density of negatively charged phospholipid molecules,<sup>18,51,52</sup> the  $\psi_0$  potential exhibits rather unexpected variations throughout monolayer compression. Figure 5B shows that even though the  $\psi_0$  potential does become more and more negative in the expanded region as the surface density of PE<sup>-</sup>-NBD groups is increased (with decreasing area per molecule upon compression), the absolute value of  $\psi_0$  starts to decrease upon onset of the  $\pi$ - $A$  isotherm plateau. This is clear evidence of a process which either affects headgroup dissociation or induces structural reorganization in the monolayer. As a result, the surface charge density at the air/water interface is altered so that the monolayer bears almost no charge in the condensed region (the  $\psi_0$  potential in Figure 5B drops from  $\sim -350$  mV at an area of 0.8 nm<sup>2</sup>/molecule to approximately  $-50$

(51) Taylor, D. M.; Oliveira, O. N., Jr.; Morgan, H. *Chem. Phys. Lett.* **1989**, *161*, 147.

(52) Aguilera, V. M.; Mafé, S.; Manzanera, J. A. *Chem. Phys. Lipids* **2000**, *105*, 225.

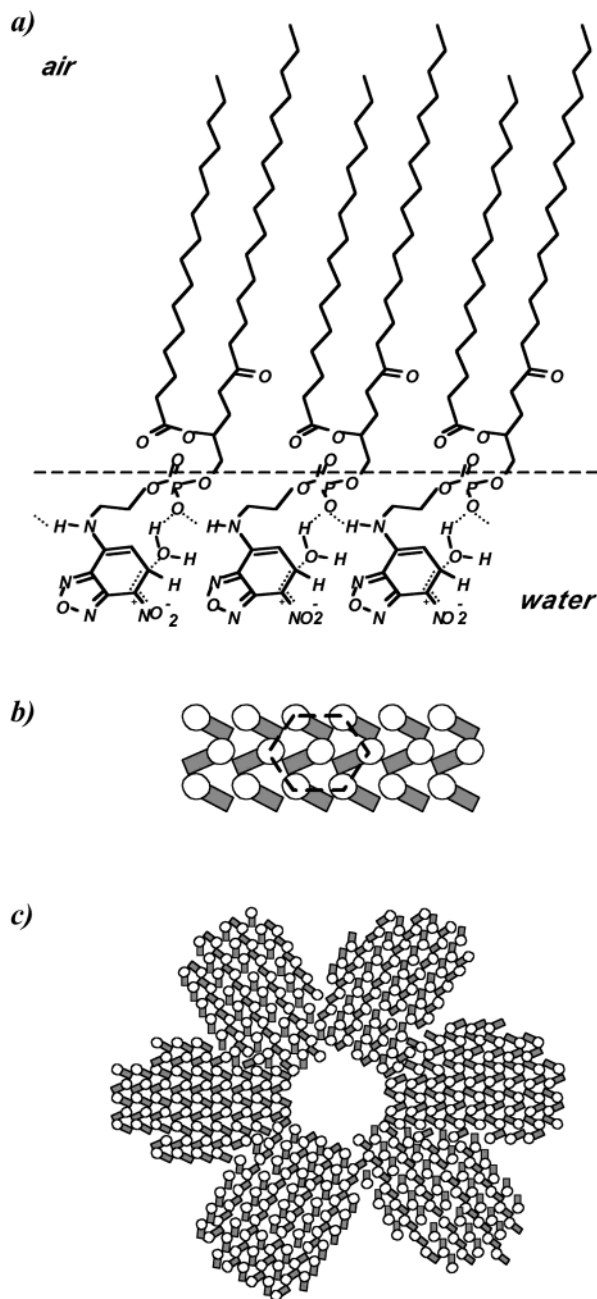


**Figure 9.** Hydrogen-bond-controlled interactions and organization of DPPE-NBD molecules in nonfluorescent rosette-shaped domains. (a) A schematic representation of the entire network of hydrogen bonds involving neighboring amino and phosphatidyl groups as well as water molecules of the  $\text{PE}^-$ -NBD hydration shell. Dotted lines illustrate interactions including hydrogen bonding and redistribution of electron density in the benzenoid ring of NBD. (b) A top view of the hexagonal packing of DPPE-NBD molecules in condensed-phase domains. Circles represent phosphatidylethanolamine headgroups, while filled blocks are NBD chromophores whose fluorescence is quenched as a result of disruption of the  $\pi$ -conjugation pathway in the benzenoid ring of NBD. (c) A top view of the packing structure in the rosette-shaped domains typically observed in the plateau region of the DPPE-NBD isotherm.

mV at the end of the isotherm). A plausible explanation considers the increasing interactions between neighboring  $\text{PE}^-$ -NBD groups occurring through networks of the hydrogen bonds as shown schematically in Figure 9a. Due to the intermolecular  $\text{H}\cdots\text{O}$  bridges, a large displacement of electron density may occur, leading to an extended delocalization of the negative charge of the phosphatidyl

group over the NBD benzofurazan ring system.<sup>1,10</sup> Eventually, the nitrogen atom of the NBD nitro group acquires a partial positive charge, while a negative charge is shared between the oxygen atoms. Thus, such intermolecular charge interactions through the hydrogen bonding involving neighboring amino and phosphatidyl groups as well as water molecules of the  $\text{PE}^-$ -NBD hydration shell are likely a reason for the decreasing negative charge of the DPPE-NBD monolayer. Moreover, these interactions can also be responsible for the observed monolayer structuring and appearance of the nonfluorescent condensed-phase domains in the plateau of the  $\pi$ -A isotherm as those in Figure 3B. Figure 9a shows that the NBD-water interactions cause a disruption of the  $\pi$ -conjugation pathway for CT between the amino group and the nitro group in the benzenoid ring of NBD and, hence, may facilitate rapid  $\text{S}_1 \rightarrow \text{S}_0$  internal conversion. Consequently, a blue shift of the absorption maximum accompanied by a red shift of the emission maximum and significant quenching of the NBD fluorescence are expected.<sup>46</sup> The fact that both these shifts and quenching were indeed observed for the DPPE-NBD monolayer at areas below  $0.8 \text{ nm}^2/\text{molecule}$  strongly supports our model of the organization of the DPPE-NBD molecules at the air/water interface. Additionally, this model is also in good agreement with the polarized fluorescence and REES data. The drawing in Figure 9a demonstrates that the entire network of intermolecular hydrogen bonds provides a regular alignment of uniformly oriented chromophores strongly interacting with each other and water molecules. This feature of the structural ordering in the DPPE-NBD monolayer requires a narrow distribution of the angle  $\theta$  like that revealed by the DPPE-NBD fluorescence anisotropy (Table 1). It also slows the rate of reorientation of the water dipoles surrounding the NBD chromophore, giving rise to REES effects such as those discussed above (Table 1). Furthermore, the complex  $\text{PE}^-$ -NBD-water interactions are of primary importance in determining the packing structure in the DPPE-NBD domains. Given that the phospholipids pack themselves in face-centered structures,<sup>34,39</sup> a packing configuration stabilizing the monolayer by the formation of ferroelectric domains may be depicted as the array in Figure 9b. It is clearly seen that the bond orientational order of  $\text{PE}^-$ -NBD groups in Figure 9b leads to a 6-fold symmetry<sup>34</sup> and, consequently, should favor formation of a hexatic solidlike phase in the DPPE-NBD monolayer. The hexatics are known to form domains of different shapes depending on the LE-LC boundary conditions.<sup>53</sup> In particular, large boundary defect line energies may initiate the growth of six petals of the rosette-like domains observed in Figure 3B whose perimeter resembles a segment of a circle<sup>53</sup> as illustrated in Figure 9c. Thus, our model of the hydrogen-bond-controlled alignment of  $\text{PE}^-$ -NBD groups is in good agreement with the observation of nonfluorescent rosette-shaped domains typical of micrographs of a DPPE-NBD monolayer in the plateau of the  $\pi$ -A isotherm.

Unfortunately, no absolute conclusions can be made on structural ordering of the NBD( $\text{C}_{12}$ )-PC molecules at the air/water interface because of a number of uncertainties associated with the interpretation of the experimental data on the NBD( $\text{C}_{12}$ )-PC monolayer. The looping of the NBD-labeled acyl chain toward water likely disrupts conventional processes for forming condensed phosphatidylcholine domains as the aliphatic chains embedded in the polar region of the NBD( $\text{C}_{12}$ )-PC monolayer hinder the interactions between the phosphatidylcholine zwitter-

(53) Fischer, T. M.; Bruinsma, R. F.; Knobler, C. M. *Phys. Rev. E* **1994**, *50*, 413.



terions. An immediate consequence is that, instead of the uniform kidney-shaped domains typical of DPPC monolayers,<sup>12</sup> the micrograph in Figure 4B exhibits irregularly distributed domains, varying in both shape and size. The complex morphology of the NBD(C<sub>12</sub>)-PC monolayer suggests that the long C<sub>12</sub> chain bearing the NBD chromophore provides more flexibility, thus allowing the NBD chromophore to adopt distinct local orientations. Presumably, more than one population of NBD chromophores exists, not characterized merely by different orientations at the air/water interface, but also experiencing different interactions with phosphatidylcholine headgroups and hydration water. As seen in Figure 4B, two kinds of condensed structures started to grow simultaneously when the monolayer was compressed to an area of 0.82 nm<sup>2</sup>/molecule. On the basis of the discussion above, one could postulate that hydrogen-bond-controlled interactions similar to those occurring in the DPPE-NBD monolayer cause the appearance of the tiny nonfluorescent circular domains while the highly fluorescent domains could result from charge-quadrupole attractions between the positive choline group and  $\pi$ -electrons of NBD.<sup>54</sup> According to Huster et al.,<sup>6</sup> cation- $\pi$  interactions determine the localization of the NBD group in the vicinity of the phospholipid headgroups. This hypothesis seems to be consistent with our spectroscopy data. Indeed, the intermolecular cation- $\pi$  interactions along the 6-fold axis of the NBD benzenoid ring are expected to reinforce the electronic attraction of the nitro group and, consequently, lead to an increase in resonance<sup>46</sup> which agrees well with the increase in the fluorescence intensity and the bathochromic shift of both absorption and emission maxima observed at areas below 0.82 nm<sup>2</sup>/molecule (see Figure 7). At the same time, though responsible for the aggregation of the NBD(C<sub>12</sub>)-PC molecule in the fluorescent domains, the cation- $\pi$  interactions do not create an entire network of rigid bonds, and hence, they allow some in-plane rotation of the NBD chromophore of NBD(C<sub>12</sub>)-PC and fast relaxation of surrounding water dipoles. This explains the lack of anisotropy in the fluorescence of NBD(C<sub>12</sub>)-PC and relatively minor REES effects.

### Conclusions

The monolayer behavior of NBD-labeled analogues of DPPE and DPPC was studied at the air/water interface by a variety of methods. Typically, a main concern about using NBD-phospholipid analogues as membrane probes is to what extent the labeling with the NBD chromophore alters the properties of native phospholipids and their interactions. Our study showed that, in contrast to the condensed-type DPPE isotherm, a liquid-expanded/liquid-condensed phase transition plateau appears in the NBD-DPPE isotherm while the NBD(C<sub>12</sub>)-PC monolayer is completely liquid-expanded, exhibiting a lack of the plateau observed in the DPPC isotherm. However, the expanded-type NBD(C<sub>12</sub>)-PC monolayer showed a rather complex morphology where two kinds of condensed structures were clearly distinguished in the homogeneous

background by fluorescence microscopy. Analysis of surface potential data revealed that, despite differences in the chemical structures of the two NBD-labeled phospholipids, the NBD group of both DPPE-NBD and NBD(C<sub>12</sub>)-PC is embedded in the headgroup region of the monolayer. In the case of acyl-chain-labeled NBD(C<sub>12</sub>)-PC, this suggests a looping of the NBD-labeled chain toward water. Spectroscopic evidence also indicates a localization of the NBD chromophore for both phospholipid compounds within the monolayer headgroup region: the positions of the absorption fluorescence maxima for NBD in these monolayers were very close to the values of absorption and fluorescence maxima of NBD in water. Moreover, Cu<sup>2+</sup> quenching experiments proved that NBD groups of NBD(C<sub>12</sub>)-PC were exposed directly to the aqueous phase. However, though localized in similar monolayer regions, the NBD chromophore of DPPE-NBD and that of NBD(C<sub>12</sub>)-PC were found to adopt distinct orientations at the air/water interface, and experience different interactions with phospholipid headgroups and surrounding water dipoles. Polarized fluorescence and REES studies supported a structural model showing regular alignment of uniformly oriented NBD chromophores in the DPPE-NBD monolayer. These oriented chromophores strongly interact with each other, phosphatidylethanolamine headgroups, and water molecules through networks of intermolecular hydrogen bonds where chromophore mobility as well as reorientational motion of water dipoles around excited-state chromophores is considerably restricted. The NBD groups of NBD(C<sub>12</sub>)-PC are also organized in condensed structures, proposed to result from intermolecular interactions provided by cation- $\pi$  electrostatic forces between the positive choline group and  $\pi$ -electrons of NBD. Nevertheless, the NBD group in these monolayers experiences a less-structured environment that permits in-plane rotation of the NBD chromophore on NBD(C<sub>12</sub>)-PC and fast relaxation of surrounding water dipoles.

Altogether, the results of the present study underscore that the monolayer behavior of the NBD-labeled phospholipids differs significantly from that of the parent phospholipids, and consequently, they should be used as analogues of natural phospholipids with caution when acyl chain conformation or motility of NBD is important. At the same time, the unique sensitivity of NBD photophysical properties to changes in local polarity and structural ordering of the environment surrounding the chromophore makes NBD-labeled analogues advantageous for the study of phospholipid organization at interfaces.

**Acknowledgment.** We thank the Natural Sciences and Engineering Research Council of Canada for the financial support of this study. C.S. is a chercheur boursier senior of the Fonds de recherche en santé du Québec. An invitation fellowship of the Centre de Recherche en Sciences et Ingénierie des Macromolécules (Quebec, Canada) to V.T. is also gratefully acknowledged.

(54) Dougherty, D. A. *Science* **1996**, 271, 163.